Volume 61
Number 19
7 March 2025
Pages 3767–3922

ChemComm

Chemical Communications

rsc.li/chemcomm

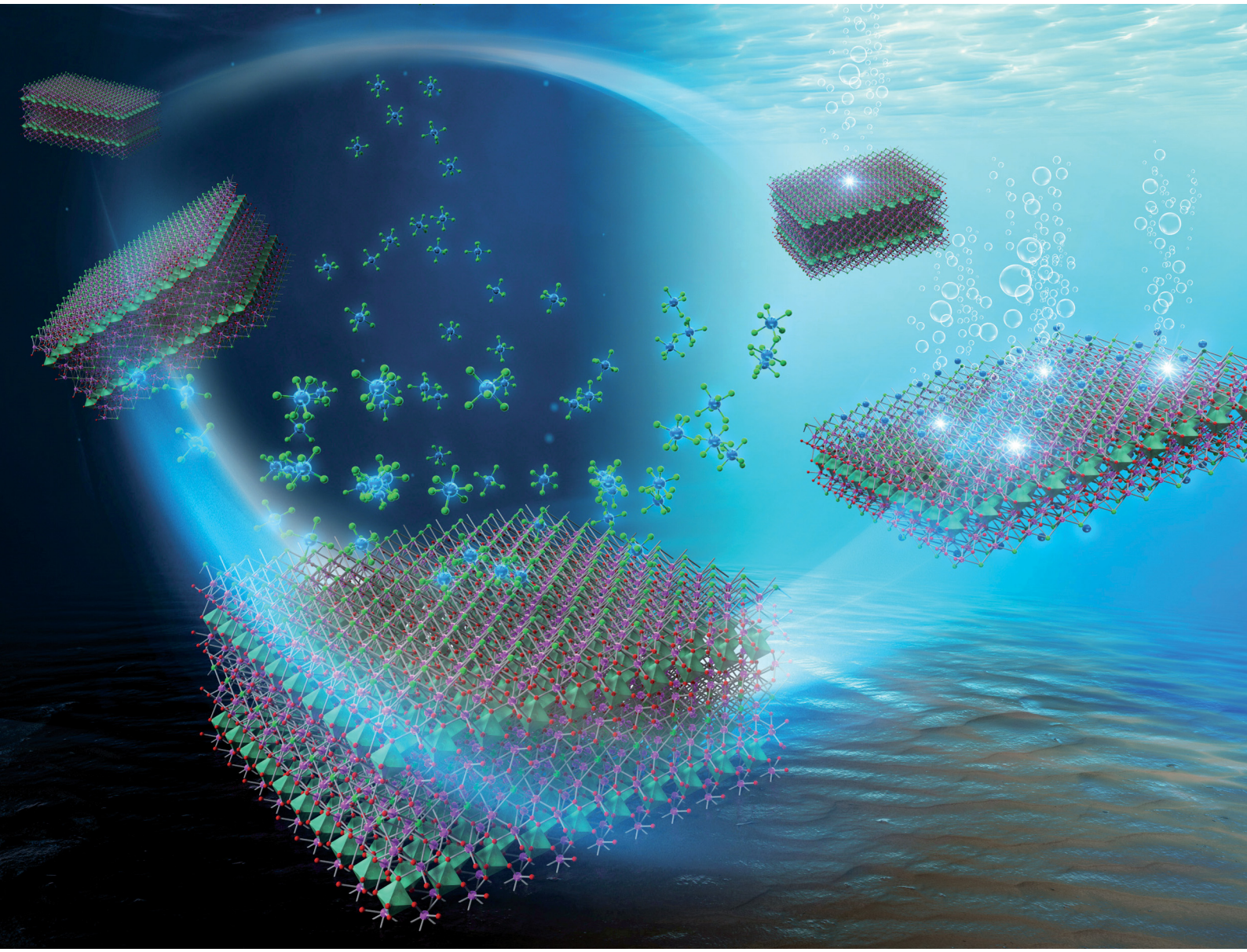

ISSN 1359-7345

ROYAL SOCIETY OF CHEMISTRY

COMMUNICATION

Hajime Suzuki, Ryu Abe *et al.*

Spontaneous adsorption of iridium chloride complex on oxychloride photocatalysts provides efficient and durable reaction site for water oxidation

ChemComm

COMMUNICATION

View Article Online
View Journal | View Issue

Check for updates

Cite this: *Chem. Commun.*, 2025, **61**, 3836

Received 22nd December 2024,
Accepted 23rd January 2025

DOI: 10.1039/d4cc06683a

rsc.li/chemcomm

Spontaneous adsorption of iridium chloride complex on oxychloride photocatalysts provides efficient and durable reaction site for water oxidation†

Hajime Suzuki, *[a] Kengo Minamimoto,[a] Yusuke Ishii, [a] Yudai Furuta,[a] Osamu Tomita, [a] Akinobu Nakada, [ab] Shunsuke Nozawa[c] and Ryu Abe *[a]

The visible-light-driven O_2 evolution on oxychloride photocatalysts, such as Bi_4NbO_8Cl, was significantly enhanced by stirring in an aqueous solution containing $IrCl_6^{3-}$ in the dark. Various characterizations indicated that highly dispersed $IrO_xH_yCl_z$-like species spontaneously formed on the oxychloride surface, serving as effective and stable cocatalysts for enhancing O_2 evolution.

Water splitting using semiconductor photocatalysts is a promising approach to clean hydrogen production.[1–5] Till now, ultraviolet (UV)-light-driven water splitting with a quantum efficiency of almost 100% has been achieved using $SrTiO_3$-based photocatalysts.[6] Large-scale photocatalytic hydrogen production tests are also underway.[7] However, since UV light accounts for only a small fraction of the solar spectrum, developing photocatalysts capable of harvesting visible light, which constitutes nearly half of sunlight, is necessary to achieve practically high efficiencies.

Mixed-anion compounds, such as oxynitrides and oxysulfides, have been developed to address this requirement.[8] These photocatalyst materials have the valence band maximum (VBM) composed of their N-2p or S-3p orbitals hybridized with O-2p. The contribution of these orbitals to the VBM reduces the bandgap and enables visible light absorption. However, these materials often suffer from self-oxidative deactivation by photogenerated holes during water splitting. Recently, Sillén-(-Aurivillius)-type layered oxyhalides, such as Bi_4NbO_8Cl, have emerged as promising photocatalysts for visible-light-driven water splitting (Fig. 1).[9,10] These materials feature a unique valence band structure, in which elevated O-2p orbitals primarily contribute to the VBM. This structure enables photogenerated holes to be preferentially consumed by water oxidation, minimizing self-oxidation and providing remarkable stability as O_2 evolution photocatalysts in Z-scheme water-splitting systems.[11,12]

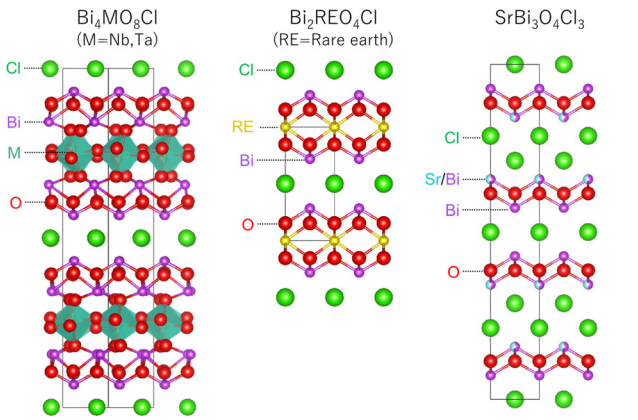

Fig. 1 Crystal structures of Sillén(-Aurivillius)-type layered oxyhalide photocatalysts: Bi_4MO_8Cl (M = Nb, Ta), Bi_2REO_4Cl (RE = rare earth), and $SrBi_3O_4Cl_3$.

Previous efforts to enhance photocatalytic activity have included the exploration of related oxyhalide materials and synthetic methods such as flux-assisted synthesis.[13,14] However, further exploration of their surface engineering is needed, particularly for loading effective water oxidation cocatalysts. Unlike the well-studied surfaces of metal oxides, layered oxyhalides possess more complex surfaces with volatile halogen species, requiring innovative surface modification strategies to improve both charge transfer and surface reactions.

While exploring effective cocatalysts and their loading methods to enhance O_2 evolution on the representative oxychloride photocatalyst Bi_4NbO_8Cl, we discovered that highly dispersed

[a] *Department of Energy and Hydrocarbon Chemistry, Graduate School of Engineering, Kyoto University, Nishikyo-ku, Kyoto 615-8510, Japan*
[b] *Precursory Research for Embryonic Science and Technology (PRESTO), Japan Science and Technology Agency (JST), 4-1-8 Honcho, Kawaguchi, Saitama 332-0012, Japan*
[c] *Photon Factory (PF), Institute of Materials Structure Science (IMSS), High Energy Accelerator Research Organization (KEK), Tsukuba, Ibaraki 305-0801, Japan*

† Electronic supplementary information (ESI) available: XRD pattern, diffuse reflectance spectrum, SEM image, photocatalytic activity, STEM image, XAFS spectrum. See DOI: https://doi.org/10.1039/d4cc06683a

$IrO_xH_yCl_z$ species were spontaneously formed by simply stirring Bi_4NbO_8Cl particles in an aqueous Na_3IrCl_6 solution in the dark. This novel adsorption method significantly enhanced the O_2 evolution rate under visible light irradiation and proved effective for various oxyhalide photocatalysts.

The oxyhalide photocatalyst Bi_4NbO_8Cl was synthesized using the previously reported flux method.[13] X-ray diffraction (XRD) analysis, scanning electron microscopy (SEM), and diffuse reflectance spectroscopy confirmed the successful synthesis of single-phase, plate-like particles of Bi_4NbO_8Cl (Fig. S1, ESI†). Initially, various metal oxide species (RuO_2, CoO_x, and IrO_2, each with 0.5 wt% metal content) were loaded onto Bi_4NbO_8Cl *via* a conventional impregnation (IMP) method. The samples were then calcinated at 450 °C in air, and their O_2 evolution activities were evaluated. As summarized in Fig. S2 (ESI†), the loading of IrO_2 provided the highest enhancement, increasing the O_2 evolution rate approximately 11-fold compared to unmodified Bi_4NbO_8Cl. RuO_2 and CoO_x also increased the rate to some extent.[13,15] Then, loading of IrO_2 cocatalysts was carried out by employing various methods, including colloidal adsorption (COL), microwave-assisted (MW) method, and photodeposition (PD) method, all of which have reportedly been effective for loading IrO_2 onto metal oxides and oxynitride photocatalysts.[16–18] Notably, the PD method was proposed to provide IrO_2 species through oxidation of $Ir^{III}Cl_6^{3-}$ precursor to $Ir^{IV}O_2$ by photogenerated holes on the photocatalyst, accompanied by nitrate ion reduction (*e.g.*, $NO_3^- + 2H^+ + 2e^- \rightarrow NO_2^- + H_2O$) by photoexcited electrons.[18]

Additionally, we introduced the simple adsorption (ADS) method as a control test for the PD method. In this approach, the photocatalyst particles were suspended in aqueous Na_3IrCl_6 solution (in the absence of NO_3^-) in the dark.

Fig. 2 shows the O_2 evolution rates of various Bi_4NbO_8Cl samples (0.1 g) in an aqueous $AgNO_3$ solution (8 mM, 100 mL) under visible light irradiation ($\lambda > 400$ nm) from a 300-W Xe-arc lamp. Among the tested methods, PD achieved the highest O_2 evolution rate, outperforming the IMP method. The COL and MW methods showed slightly higher rates than the bare sample but considerably lower values than IMP. Notably, the newly introduced ADS method, in which Bi_4NbO_8Cl particles were stirred in an aqueous Na_3IrCl_6 solution under dark conditions, achieved a rate comparable to that of PD, the highest among all the methods. The O_2 evolution rate of the ADS sample remained steady until the Ag^+ ions in the solution were completely consumed (Fig. S3, ESI†). Attempts to apply the ADS method with other metal species (*e.g.*, Ru and Co) did not significantly enhance the O_2 evolution rates (Fig. S4, ESI†), indicating that the enhancement is unique to the Ir species. The ADS sample also exhibited higher activity than the bare sample, not only with the sacrificial electron acceptors (Ag^+) but also with the reversible electron acceptors (Fe^{3+} and polyoxometalate $[SiV^VW_{11}O_{40}]^{5-}$) (Fig. S5, ESI†). These findings highlight the potential of such modified oxyhalide photocatalysts in Z-scheme water-splitting systems with redox mediators.

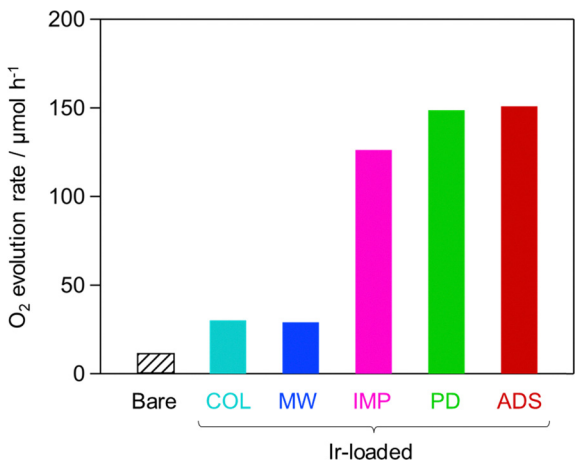

Fig. 2 Initial O_2 evolution rate of Bi_4NbO_8Cl loaded with Ir species *via* various methods (COL, MW, IMP, PD, and ADS), along with that of bare Bi_4NbO_8Cl. These reactions were performed in aqueous $AgNO_3$ solution (8 mM, 100 mL) containing the photocatalyst powder (0.1 g) under visible light irradiation ($\lambda > 400$ nm) from a 300-W Xe-arc lamp.

The Ir species loaded *via* ADS and other methods were characterized using various techniques. Inductively coupled plasma (ICP) spectroscopy measurements indicated that most of the introduced Ir species (0.5 wt% metal content) were successfully loaded onto the surface of Bi_4NbO_8Cl, regardless of the loading method (Fig. S6, ESI†). The driving force for the spontaneous adsorption of Ir species is likely related to the electrostatic attraction between the Bi_4NbO_8Cl particles and the $IrCl_6^{3-}$ precursor. The pH of the solution during the ADS method was measured to be around 5. At pH 5, the Bi_4NbO_8Cl particles are positively charged,[19] suggesting that the electrostatic attraction between them possibly promotes the adsorption of Ir species. Fig. 3 and Fig. S7 (ESI†) show scanning transmission electron microscope (STEM) images of each Bi_4NbO_8Cl sample. For the ADS sample (Fig. 3), identifying the Ir species was almost impossible, suggesting highly dispersed, fine particles or clusters on the surface. Alternatively, Ir species are distinctly evident in the MW sample but are indistinguishable in the PD sample, as shown in Fig. S7 (ESI†). The IMP sample exhibited much smaller Ir species compared to those from the MW and COL methods. These observations imply that Ir species with high dispersion and small size are critical for enhancing O_2 evolution on Bi_4NbO_8Cl photocatalysts.

The X-ray absorption fine structure (XAFS) results are shown in Fig. 4 and Fig. S8 (ESI†). The X-ray absorption near-edge structure (XANES) spectra (Fig. S8, ESI†) revealed that the loaded Ir species predominantly existed in the +4 oxidation state across all loading methods. In the extended XAFS (EXAFS) spectra (Fig. 4), the Ir species loaded using the COL, MW, and IMP methods showed only Ir–O bonds in the first coordination shell, indicating that the Ir species existed as oxides or hydroxides, as previously reported. In contrast, the samples prepared *via* ADS and PD methods exhibited both Ir–O and Ir–Cl bonds, indicating the formation of $IrO_xH_yCl_z$ species, which are effective cocatalysts for O_2 evolution. The PD method was originally proposed to deposit IrO_2 on a photocatalyst through the oxidation of $IrCl_6^{3-}$ by photogenerated holes, accompanied by the

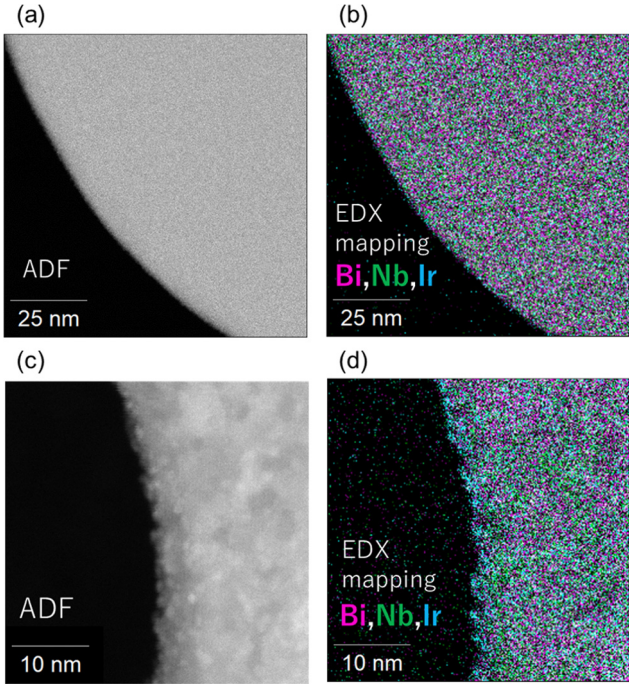

Fig. 3 (a) and (c) STEM image and (b) and (d) EDX mapping of Bi_4NbO_8Cl loaded with Ir species *via* ADS (a) and (b) and MW (c) and (d) method.

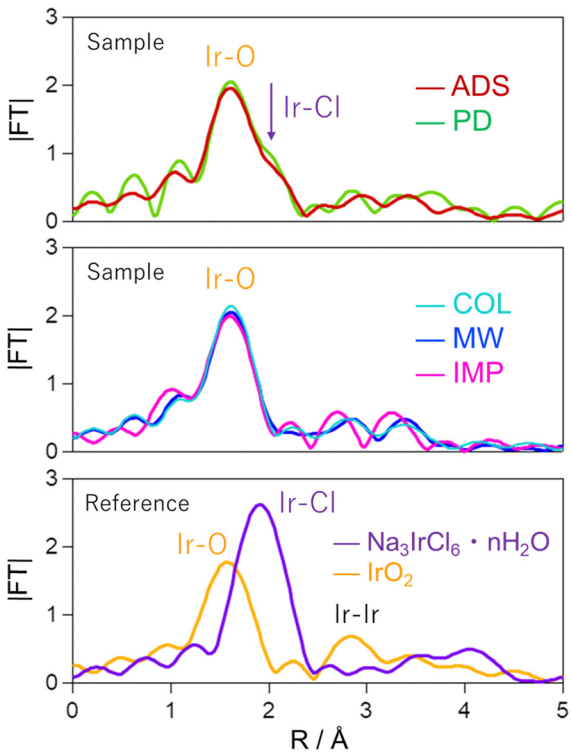

Fig. 4 Fourier-transformed Ir L_3-edge EXAFS spectra of Bi_4NbO_8Cl loaded with Ir species *via* various methods (COL, MW, IMP, PD, and ADS), along with those of reference samples.

reduction of NO_3^- by photoexcited electrons under light irradiation.[18] However, the present ADS method achieved comparably high activity than the PD method without light or electron acceptor. Additionally, the states of the Ir species loaded *via* ADS and PD were almost identical, as confirmed by STEM and XAFS measurements. Thus, for both methods, the $IrO_xH_yCl_z$ species are probably loaded on the oxyhalide through the partial hydrolysis of $IrCl_6^{3-}$ in water.[20,21] Notably, the EXAFS spectrum of the ADS-loaded sample post-photocatalytic O_2 evolution still showed Ir–Cl bonds, indicating stability under the photocatalytic reaction conditions (Fig. S9, ESI†). These findings indicate that active Ir species were spontaneously formed from $IrCl_6^{3-}$ on the Bi_4NbO_8Cl surface during stirring in the dark, for both the PD and ADS methods.

We applied this novel ADS method to other oxychloride photocatalysts, including Bi_4TaO_8Cl, Bi_2ErO_4Cl, and $SrBi_3O_4Cl_3$ (Fig. 1 and Fig. S10, ESI†). Fig. 5 shows the O_2 evolution rates of these oxyhalide photocatalysts with Ir species loaded using the ADS method. The time course of O_2 evolution is shown in Fig. S11 (ESI†). Ir loading significantly improved the O_2 evolution rates for both Sillén-type (Bi_2ErO_4Cl and $SrBi_3O_4Cl_3$) and Sillén-Aurivillius-type (Bi_4NbO_8Cl and Bi_4TaO_8Cl) oxychlorides. In contrast, applying the ADS method to oxide-based ($BiVO_4$ and WO_3) and oxynitride-based (TaON) photocatalysts negligibly improved the O_2 evolution (Fig. S12, ESI†). This distinction indicates that the $IrCl_6^{3-}$ complex possibly interacts with the surface of oxychlorides, facilitating the formation of highly active Ir species and/or enabling efficient charge transfer, thereby significantly enhancing O_2 evolution rates. As shown in Fig. S13 (ESI†), using Na_2IrCl_6 significantly enhances O_2 evolution similar to Na_3IrCl_6 on Bi_4NbO_8Cl, whereas Ir(acac)$_3$ without Cl anions yields less pronounced improvement. These findings underscore the critical role of surface Cl interactions on oxychlorides. Further investigation is required to elucidate the mechanisms underlying this activity enhancement. Nonetheless, the novel ADS method is a mild, simple, and versatile method for loading active and stable Ir species, significantly enhancing the O_2 evolution rates of various oxychloride photocatalysts.

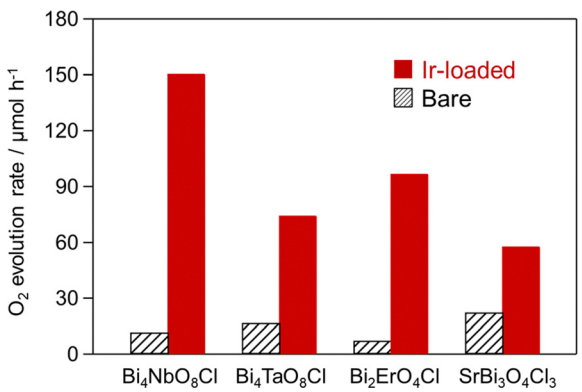

Fig. 5 Initial O_2 evolution rate of oxyhalides loaded with or without Ir species *via* ADS method. These reactions were performed in aqueous $AgNO_3$ solution (8 mM, 100 mL) containing the photocatalyst powder (0.1 g) under visible light irradiation ($\lambda > 400$ nm) from a 300-W Xe-arc lamp.

In summary, this study demonstrated the potential of the novel ADS method as a simple, mild, and versatile approach for enhancing the visible-light-driven O_2 evolution activity of oxyhalide photocatalysts by loading highly dispersed and active Ir species. This method effectively improved the performance of not only a representative oxyhalide Bi_4NbO_8Cl but also of various other oxyhalide photocatalysts through simple stirring in an aqueous Ir precursor solution. The success of the ADS method, particularly with oxyhalides rather than with conventional oxides and oxynitrides, suggests the importance of Cl-mediated interactions in facilitating effective cocatalyst deposition and/or charge transfer. These findings provide valuable insights for the development of tailored cocatalysts and their loading techniques to optimize the photocatalytic efficiency of mixed-anion photocatalysts.

This work was supported by JSPS KAKENHI (JP20H00398 and JP23H02061) through Grants-in-Aid for Scientific Research (A) and (B), respectively. This study was also supported by the JSPS Core-to-Core Program (JPJSCCA20200004), Kansai Research Foundation for Technology Promotion, and ENEOS Tonengeneral Research/Development Encouragement & Scholarship Foundation. Part of this study was supported by the Advanced Characterization Platform and AIST Nanocharacterization Facility (ANCF) Platform as a program of the "Nanotechnology Platform" (JPMXP1223 KU0001). The XAFS experiments were performed with the approval of the Photon Factory Program Advisory Committee (Proposal No. 2024G638). The authors would like to acknowledge Dr Rie Haruki of the High Energy Accelerator Research Organization (KEK) for assistance with the XAFS measurements. We are also grateful to Mr Takaaki Toriyama of Kyushu University for his support with STEM analysis.

Data availability

The data supporting this article have been included as part of the ESI.†

Conflicts of interest

There are no conflicts to declare.

Notes and references

1 A. Fujishima and K. Honda, *Nature*, 1972, **238**, 37–38.
2 A. Kudo and Y. Miseki, *Chem. Soc. Rev.*, 2009, **38**, 253–278.
3 R. Abe, *Bull. Chem. Soc. Jpn.*, 2011, **84**, 1000–1030.
4 F. E. Osterloh, *Chem. Soc. Rev.*, 2013, **42**, 2294–2320.
5 S. S. Chen, T. Takata and K. Domen, *Nat. Rev. Mater.*, 2017, **2**, 17050.
6 T. Takata, J. Jiang, Y. Sakata, M. Nakabayashi, N. Shibata, V. Nandal, K. Seki, T. Hisatomi and K. Domen, *Nature*, 2020, **581**, 411–414.
7 H. Nishiyama, T. Yamada, M. Nakabayashi, Y. Maehara, M. Yamaguchi, Y. Kuromiya, H. Tokudome, S. Akiyama, T. Watanabe, R. Narushima, S. Okunaka, N. Shibata, T. Takata, T. Hisatomi and K. Domen, *Nature*, 2021, **598**, 304–307.
8 A. Miyoshi and K. Maeda, *Solar RRL*, 2020, **5**, 2000521.
9 H. Fujito, H. Kunioku, D. Kato, H. Suzuki, M. Higashi, H. Kageyama and R. Abe, *J. Am. Chem. Soc.*, 2016, **138**, 2082–2085.
10 H. Suzuki, H. Kunioku, M. Higashi, O. Tomita, D. Kato, H. Kageyama and R. Abe, *Chem. Mater.*, 2018, **30**, 5862–5869.
11 H. Kunioku, M. Higashi, O. Tomita, M. Yabuuchi, D. Kato, H. Fujito, H. Kageyama and R. Abe, *J. Mater. Chem. A*, 2018, **6**, 3100–3107.
12 D. Kato, K. Hongo, R. Maezono, M. Higashi, H. Kunioku, M. Yabuuchi, H. Suzuki, H. Okajima, C. C. Zhong, K. Nakano, R. Abe and H. Kageyama, *J. Am. Chem. Soc.*, 2017, **139**, 18725–18731.
13 K. Ogawa, A. Nakada, H. Suzuki, O. Tomita, M. Higashi, A. Saeki, H. Kageyama and R. Abe, *ACS Appl. Mater. Interface*, 2019, **11**, 5642–5650.
14 Y. Ishii, H. Suzuki, K. Ogawa, O. Tomita, A. Saeki and R. Abe, *Sustainable Energy Fuels*, 2022, **6**, 3263–3270.
15 S. Chang, L. Shi, J. Yu, R. Wang, X. Xu and G. Liu, *Appl. Catal., B*, 2023, **328**, 122541.
16 K. Maeda and K. Domen, *Angew. Chem., Int. Ed.*, 2012, **51**, 9865–9869.
17 K. Chen, J. Xiao, J. J. M. Vequizo, T. Hisatomi, Y. Ma, M. Nakabayashi, T. Takata, A. Yamakata, N. Shibata and K. Domen, *J. Am. Chem. Soc.*, 2023, **145**, 3839–3843.
18 A. Iwase, H. Kato and A. Kudo, *Chem. Lett.*, 2005, **34**, 946–947.
19 K. Ogawa, R. Sakamoto, C. Zhong, H. Suzuki, K. Kato, O. Tomita, K. Nakashima, A. Yamakata, T. Tachikawa, A. Saeki, H. Kageyama and R. Abe, *Chem. Sci.*, 2022, **13**, 3118–3128.
20 J. C. Chang and C. S. Garner, *Inorg. Chem.*, 1965, **4**, 209–215.
21 K.-C. Tso, T.-Y. Chan, T.-C. Yu, Y.-J. Tao, C.-Y. Chu, S.-Y. Chen, J.-F. Lee, J. Ohta, P.-C. Chen and P.-W. Wu, *Surf. Interfaces*, 2024, **44**, 103785.